Brüel & Kjær application notes

Mobility and loss-factors of floors using dual channel analysis

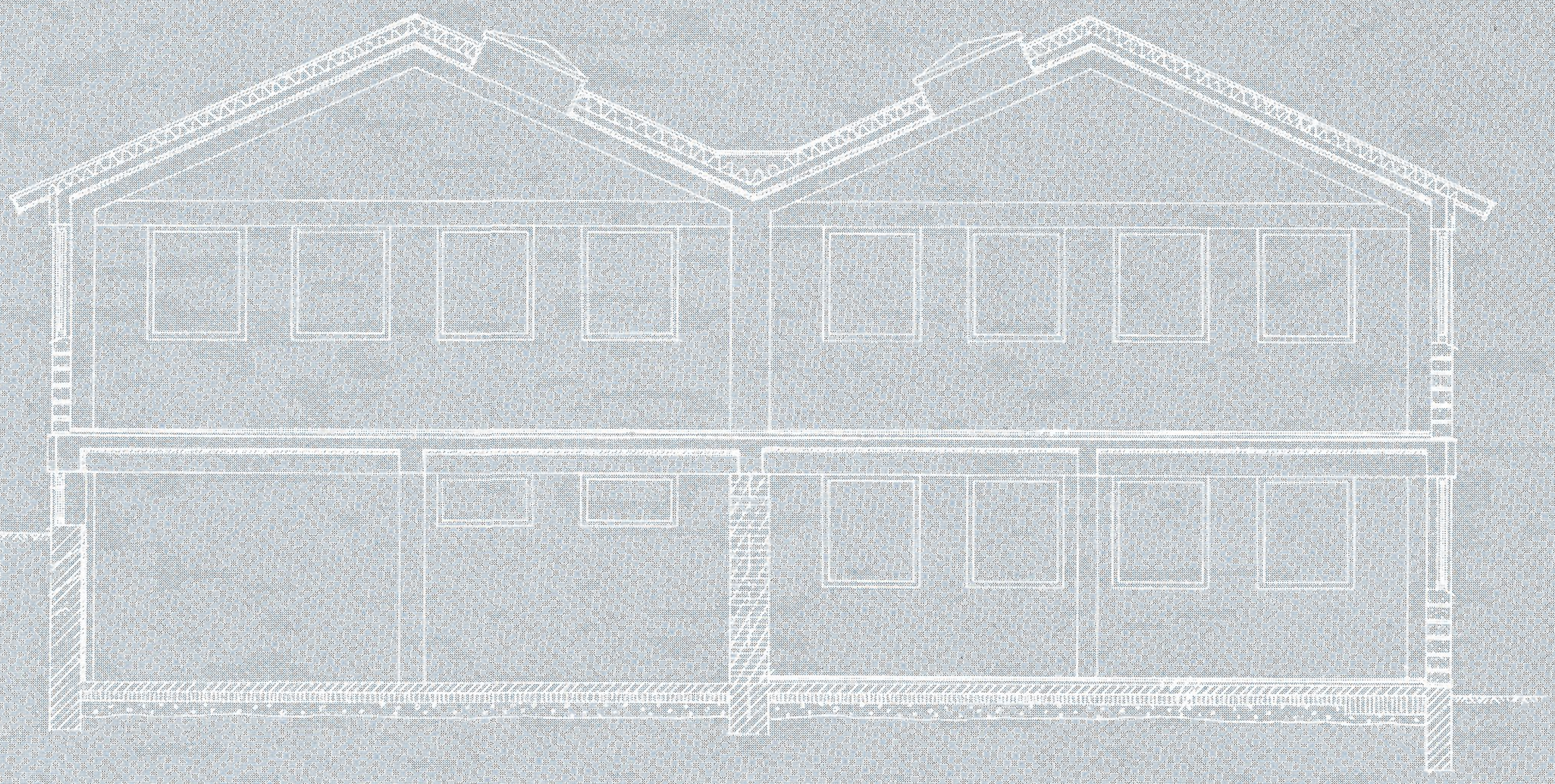

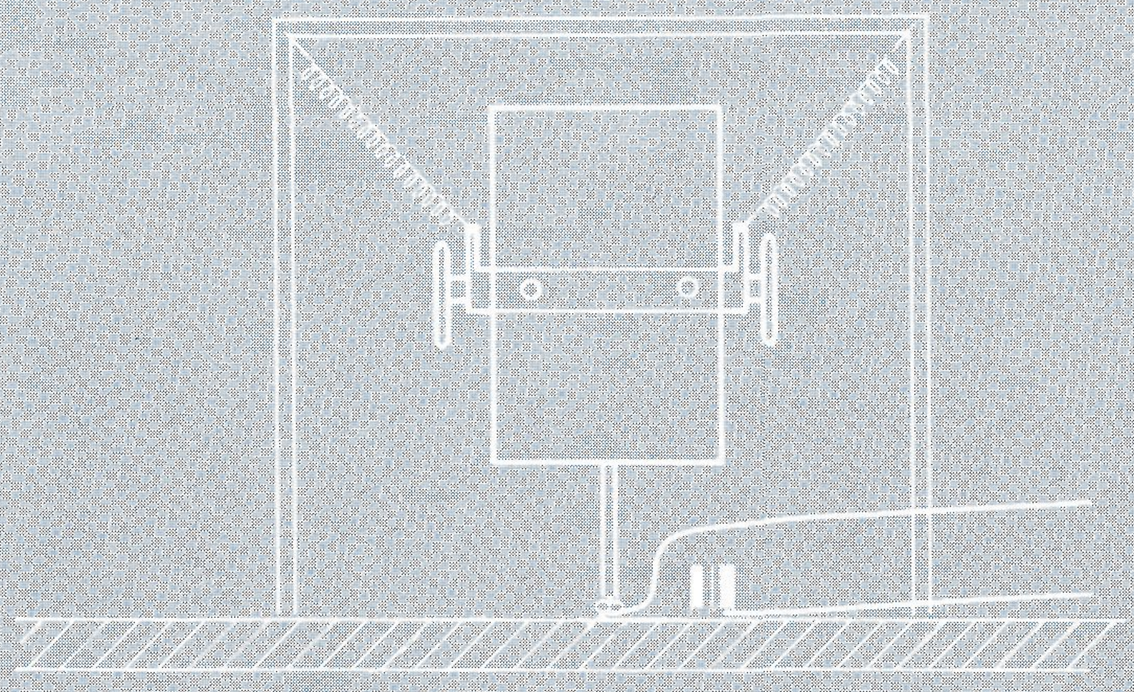

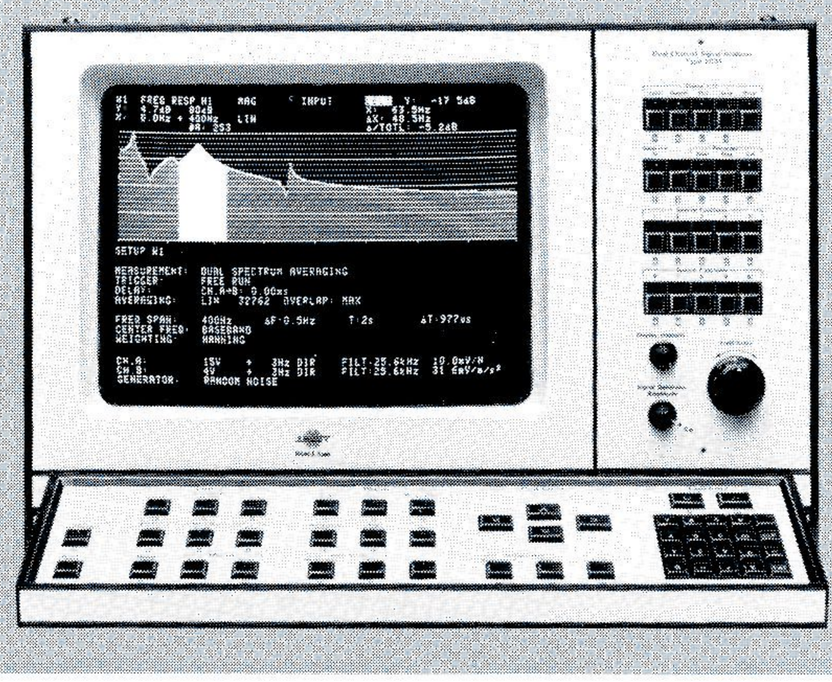

Mobility and loss factor of floors using dual channel analysis

by *K.B.Ginn & H.Herlufsen*

Objective

The aim of this note is to demonstrate the ease with which a Dual Channel Signal Analyzer Type 2032 or Type 2034 can be used to gather the necessary mobility (velocity-/force) and loss factor data used in the prescription of an isolator system. The analyser was used to measure point and transfer mobilities and loss factor (damping) on a floor in a factory workshop using vertical translational excitation [1],[2]. Standard methods for the experimental determination of mechanical mobility are described in [3] to [7].

The use of mobility measurements

Machinery installed in buildings can give rise to unacceptable noise and vibration levels. This is particularly true for many modern buildings where the trends are towards lightweight structures and longer floor spans. If the annoyance from machinery installations can be anticipated at the design stage then some type of vibration isolation system could be prescribed. In principle, design engineers require information about the nature of the excitation and the dynamic characteristics of both the machine and the building structure. In practice, the choice of vibration isolation systems usually depends on previous experience, backed by mathematical modelling of the machine / isolator / floor assembly and by use of commercial design charts.

Simplified theory of mobility

An exact description of the dynamics of even a simple machine / isolator / floor assembly would be very complex because in general, each isolator under a machine has not one but 6 degrees of freedom (3 translational and 3 rotational). For an isolator which can be considered as massless (i.e. for frequencies at which the inertia effects of the isolator are negligible), the forces at each end of the isolator are equal and opposite and the modified transmissibility T_m is:

$$T_m = M_R / (M_S + M_I + M_R)$$

and the isolator effectiveness E is:

$$E = 1 + M_I / (M_S + M_R)$$

where M_I, M_S and M_R are the isolator, source and receiver mobilities respectively which are complex functions [8] (see Fig.1). These equations show that source and receiver mobilites must be known if an isolator is to be chosen to give the required transmissibility. Furthermore, for good isolation:

$$M_I \gg M_S + M_R$$

If the foundation is very rigid then $M_R \ll M_I$ and $M_R \ll M_S$. In this case, good isolation is obtained for $M_I \gg M_S$. Many noise reduction calculations are based on this assumption for want of better information. Insertion losses obtained in practice are often considerably lower than the theoretically predicted values. The reason could be that other degrees of freedom are neglected but in many cases it is caused by the simplification mentioned above [9].

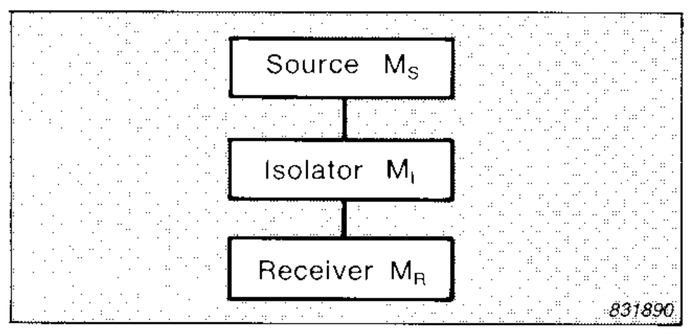

Fig. 1. A simple model of a source, isolator and receiver assembly each component possessing a mobility of M_S M_I M_R respectively

Instrumentation

The measurement system (Fig.2) was easy to install and the measurements themselves were quickly performed and thus the disruption caused in the workshop was kept to a minimum. The random excitation signal was taken directly from the Dual Channel Signal Analyzer. An

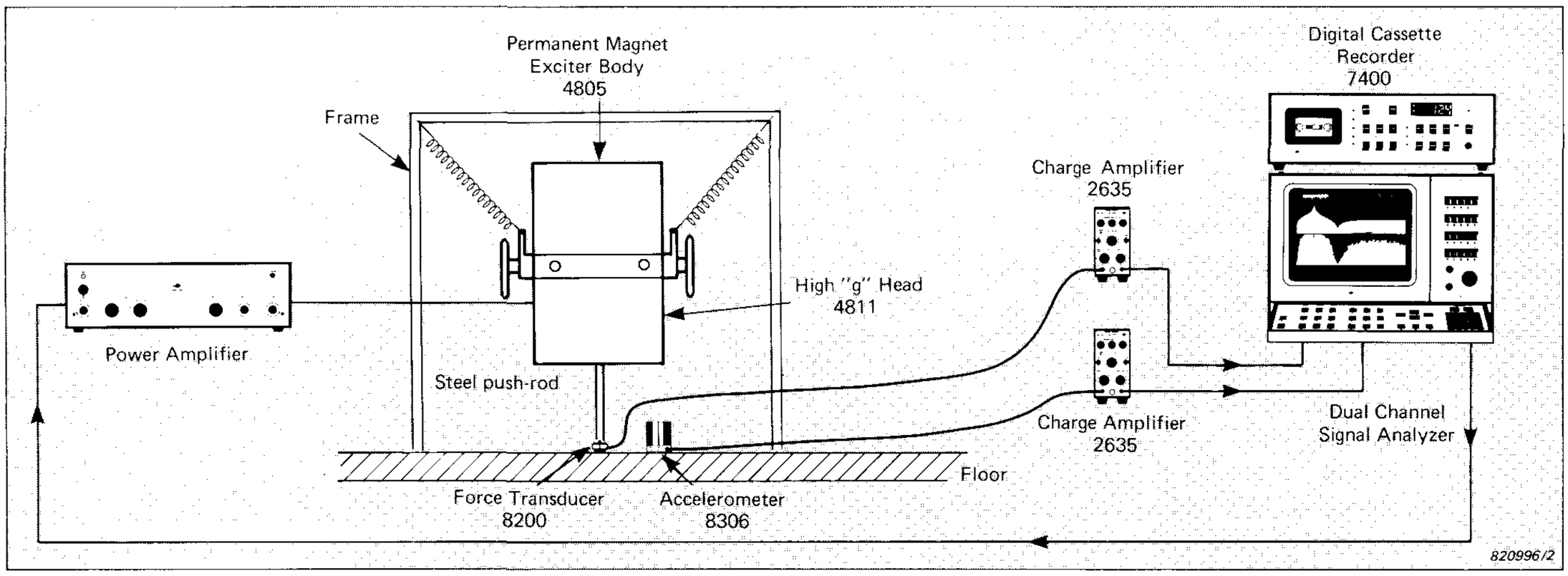

Fig. 2. Measurement system. As the velocity signals on some floors were very weak, a High Sensitivity Accelerometer Type 8200 had to be employed

electrodynamic vibration exciter was coupled via a push-rod to a force transducer which made contact with the floor via a hemispherical steel tip. The whole assembly was supported by springs in a frame. A high sensitivity, low frequency accelerometer was fixed, using double–sided tape, as close to the measurement point as possible [2].

All measurement data were stored on a Digital Cassette Recorder Type 7400 (about 20 data sets per cassette) for later post-processing by the Dual Channel Signal Analyzer. Hard copies of mobility curves, coherence functions, Nyquist plots etc., were traced out using a Graphics Recorder Type 2313. An X–Y Recorder Type 2308 could also have been used (see Fig.3).

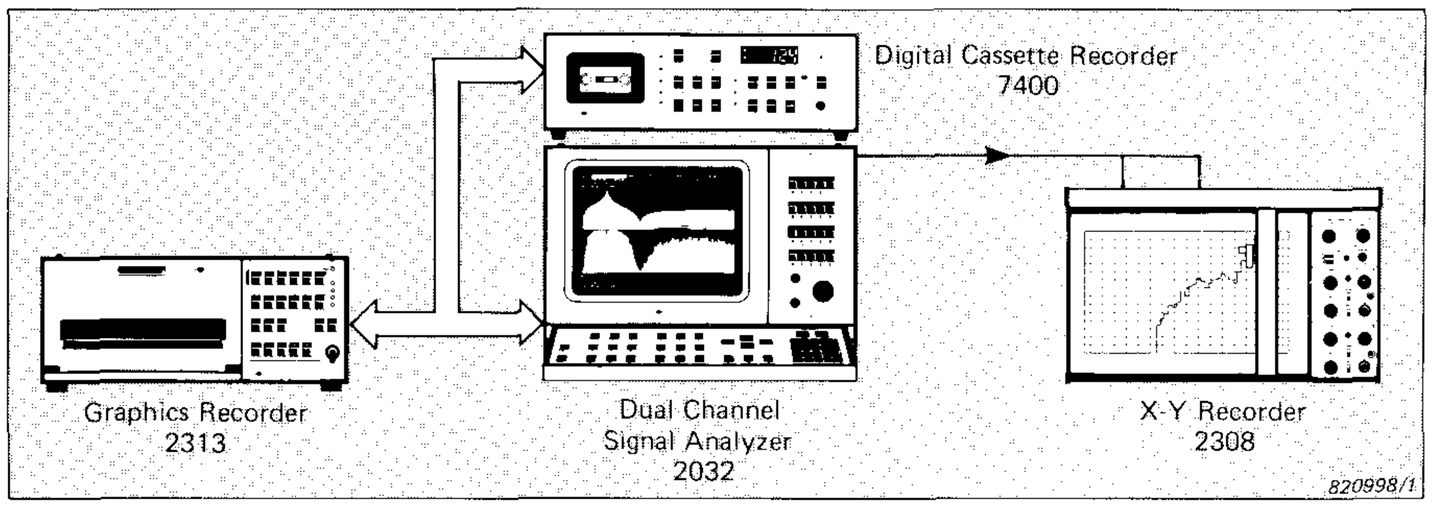

Fig. 3. Data flow possibilities. Measured spectra recorded on the Digital Cassette Recorder Type 7400 may be reintroduced into the Dual Channel Analyzer for post-processing. Hard copies of the results may be obtained from the Graphics Recorder or from the X-Y Recorder

The floor

The floor on which the measurements were performed was the first floor of a two-storey building (see line drawing on front cover). The span of the floor between supporting columns was 4,15 m. The floor consisted of 20 cm reinforced concrete with 3×3 cm battens laid at 40 cm intervals which were overlaid with beechwood floor boards. The dimensions of the floor were approximately 10×20 m and it was unevenly loaded with workbenches and goods-crates.

Practical aspects of mobility measurements

For practical mobility measurements there are several important requirements which must be observed such as calibration and tests for the validity of results (e.g. coherence, linearity, reciprocity) [3],[4]. For the purpose of these demonstration measurements these requirements were not strictly adhered to.

Calibration

The measurement system should be calibrated by measuring either the mobility (velocity / force) or the accelerance (acceleration / force) of a freely suspended rigid calibration block of known mass. (Accelerance is also commonly known as inertance). The mass of the calibration block should be selected so that its mobility is representative of the mobilites to be measured. As an indication of the type of block used in practice, one can mention that Fahy & Westcott [1] used a concrete calibration block with a mass of 224 kg.

Coherence

Mathematically the coherence function $\gamma^2(f)$ is defined as:

$$\gamma^2(f) = |G_{AB}(f)|^2 / G_{AA}(f)\, G_{BB}(f)$$

where
$|G_{AB}(f)|^2$ is the square of the magnitude of the cross spectrum between the excitation signal and the response signal.
$G_{AA}(f)$ is the input autospectrum.
$G_{BB}(f)$ is the output autospectrum.

By definition, the value of the coherence function lies between zero and unity.

When using a non-sinusoidal excitation, the coherence function between the excitation signal and the response signal should always be computed as a check on certain potential errors in the computed frequency response. In ANSI S2.32-1982 a set of curves are given which relate the computed coherence function, the number of spectra averaged and the random error. A sufficient number of spectra should be averaged to achieve at least 90% confidence so that the random error in the computed driving-point mobility is less than 5%. At least the same number of spectra should be averaged when computing the corresponding transfer mobilities. For the measurements discussed in this note the random error was less than 2%.

Linearity

A check should be made to detect non-linear effects by measuring the frequency response then repeating the measurement using significantly increased or decreased excitation amplitude [4].

For the measurements discussed here, the excitation amplitude was set to give acceptable levels at the force transducer and the accelerometer. The autospectra and the frequency response functions were measured at this excitation amplitude, and then at amplitudes 12 dB higher and 8 dB lower. As the measured spectra were practically identical at all three excitation levels, the system could be assumed to behave linearly at the medium excitation level.

Reciprocity

The principle of dynamic reciprocity requires equality between corresponding pairs of transfer mobilities for linear elastic structures [4]. In simple words the principle states that the ratio of the velocity measured at point A to the force measured at point B, should be equal to the ratio of the velocity measured at point B to the force measured at point A. In symbolic notation this statement may be written $V_A / F_B = V_B / F_A$ or $M_{AB} = M_{BA}$. Agreement between such pairs of measurements for a given linear structure confirms that proper test equipment and procedures are being used [4,11]. Reciprocity, however, might also occur in non-linear systems e.g. a perfectly symmetrical

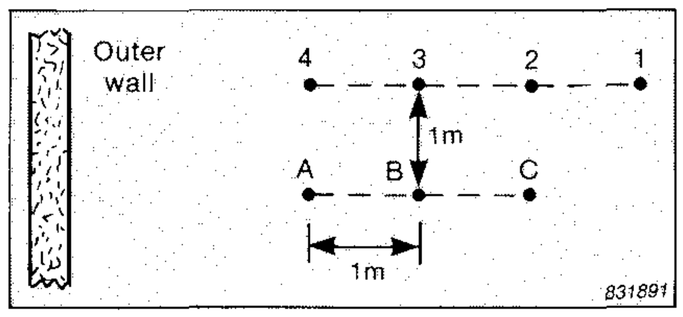

Fig. 4. Relative positions of the measurement points

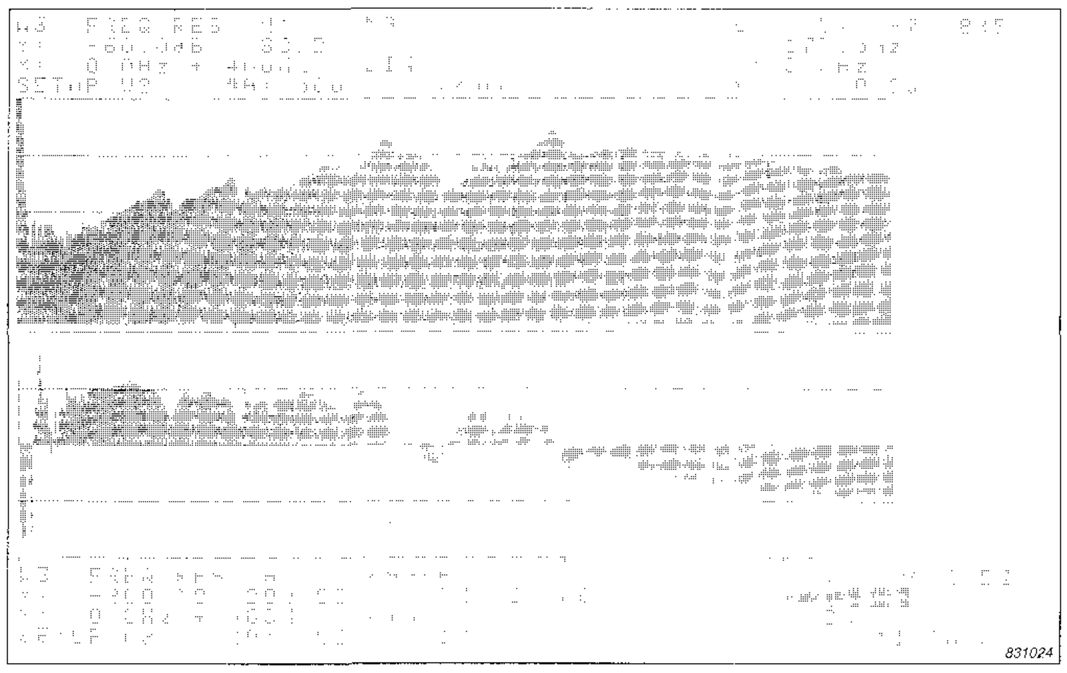

Fig. 5. Magnitude and phase of point mobility M_{AA} on a linear frequency scale from 0 Hz to 400 Hz

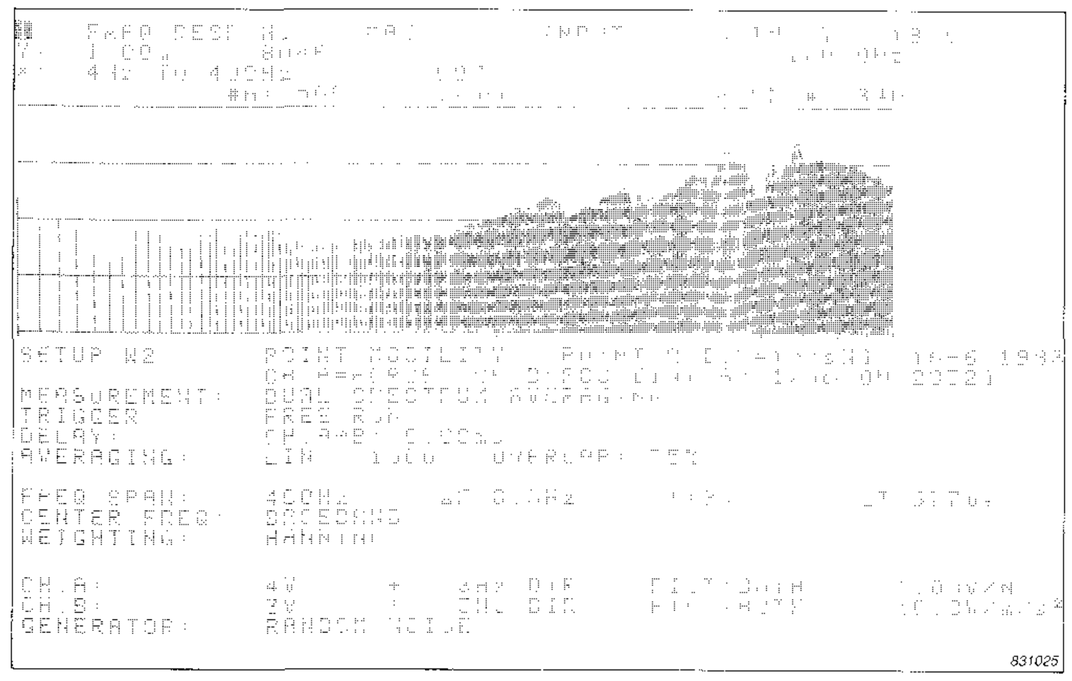

Fig. 6. Magnitude of point mobility M_{AA} on a logarithmic frequency scale from 4 Hz to 400 Hz. Measurement set-up is also shown

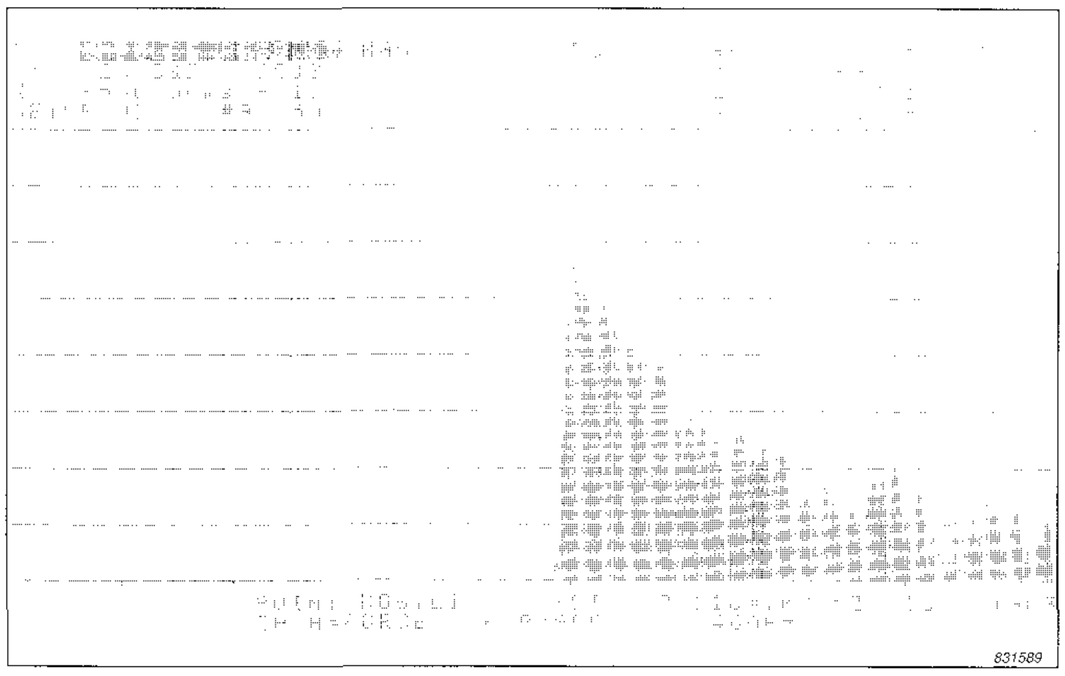

Fig. 7. Magnitude of the impulse response at point A

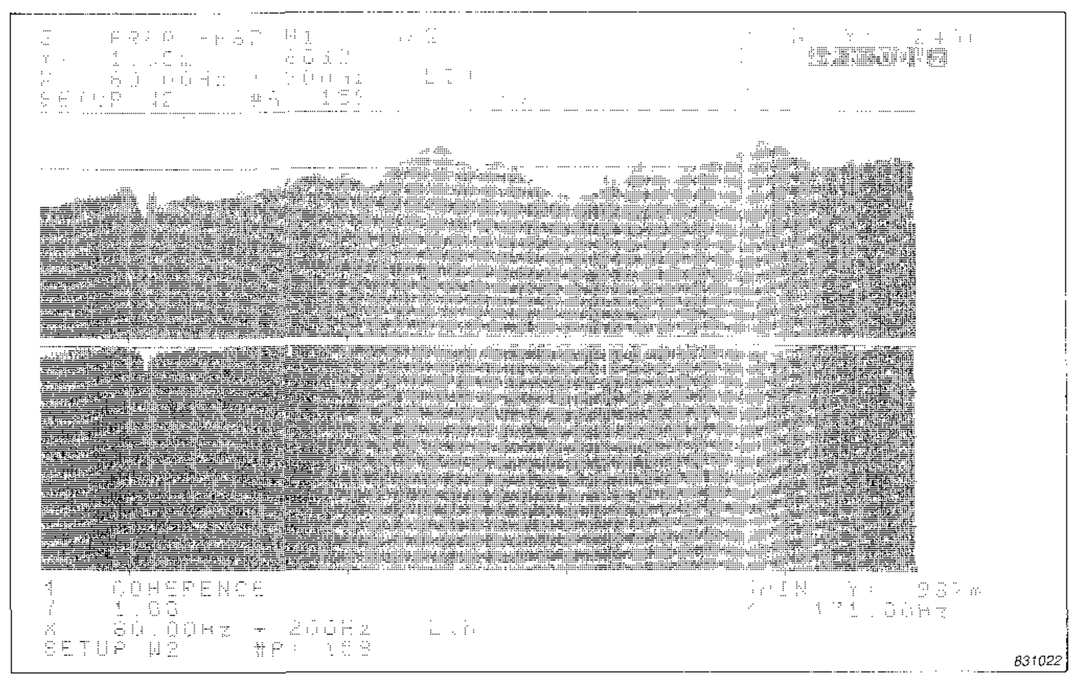

Fig. 8. Magnitude and coherence of point mobility M_{AA} on a linear frequency scale from 80 Hz to 280 Hz

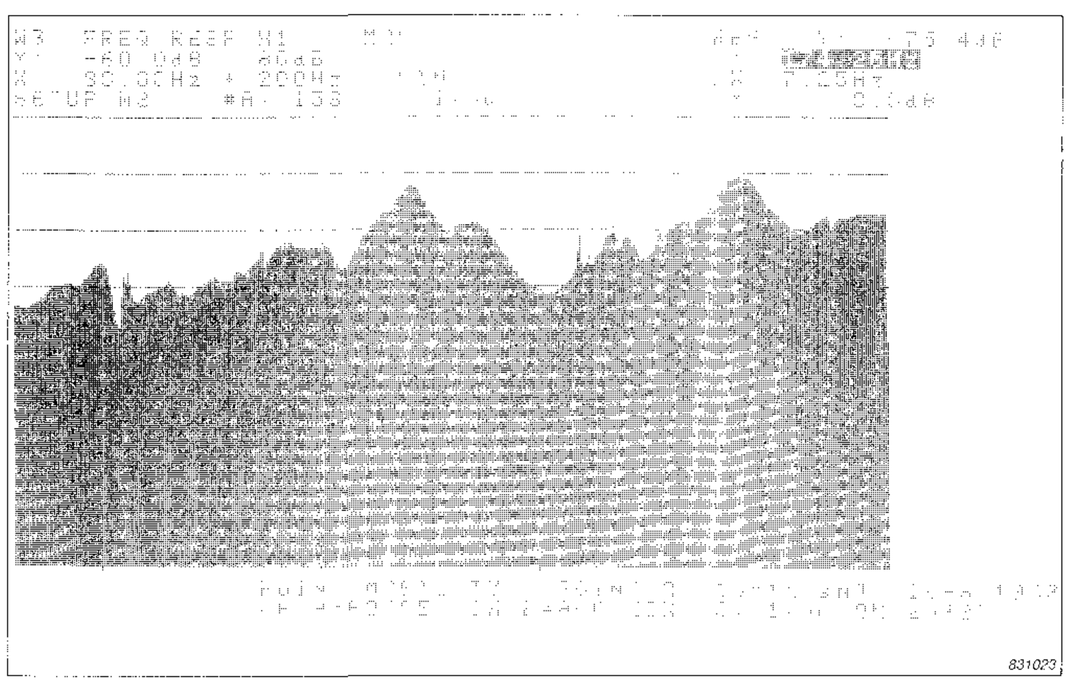

Fig. 9. Magnitude of point mobility M_{AA} in full format on a linear frequency scale from 80 Hz to 280 Hz

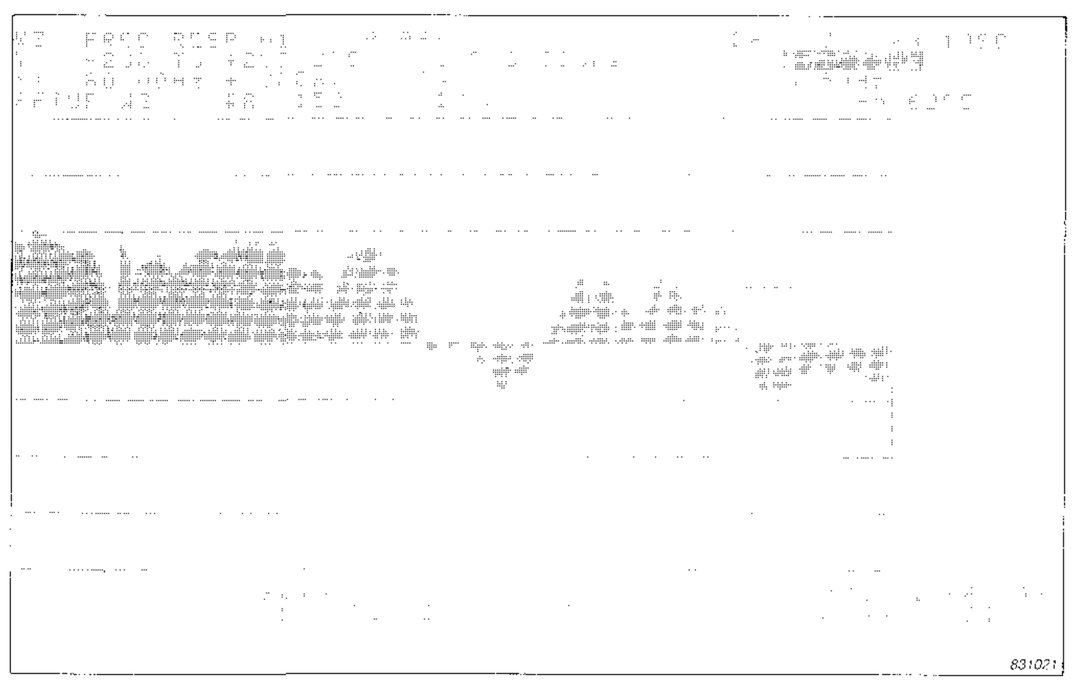

Fig. 10. Phase for point mobility M_{AA} in full format on a linear frequency scale from 80 Hz to 280 Hz

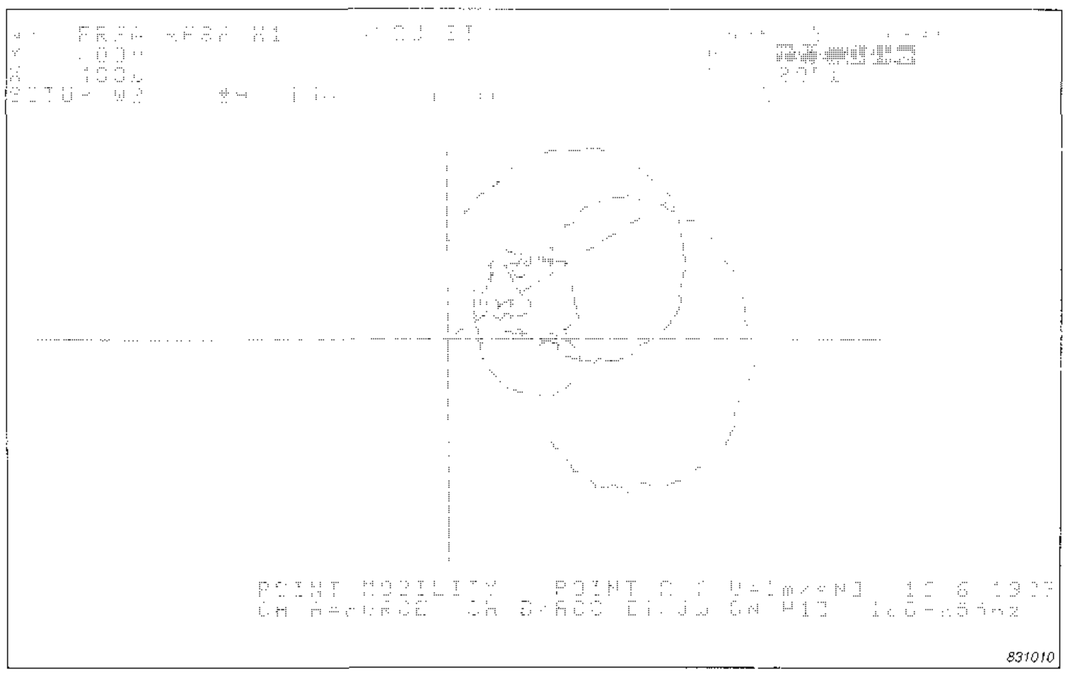

Fig. 11. Nyquist plot for point A from 160 Hz to 255 Hz. The large arcs correspond to the principal resonances at 171 Hz and 246 Hz

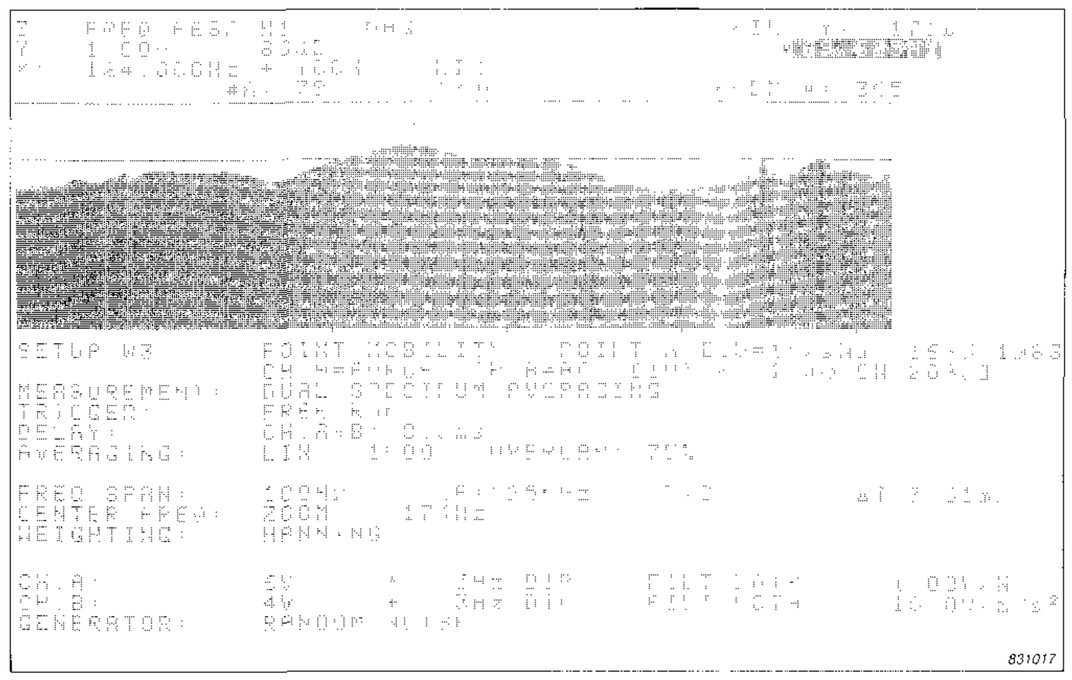

Fig. 12. Zoomed point mobility M_{AA}. Magnitude on a linear frequency scale from 124 Hz to 224 Hz. Measurement set-up is also shown

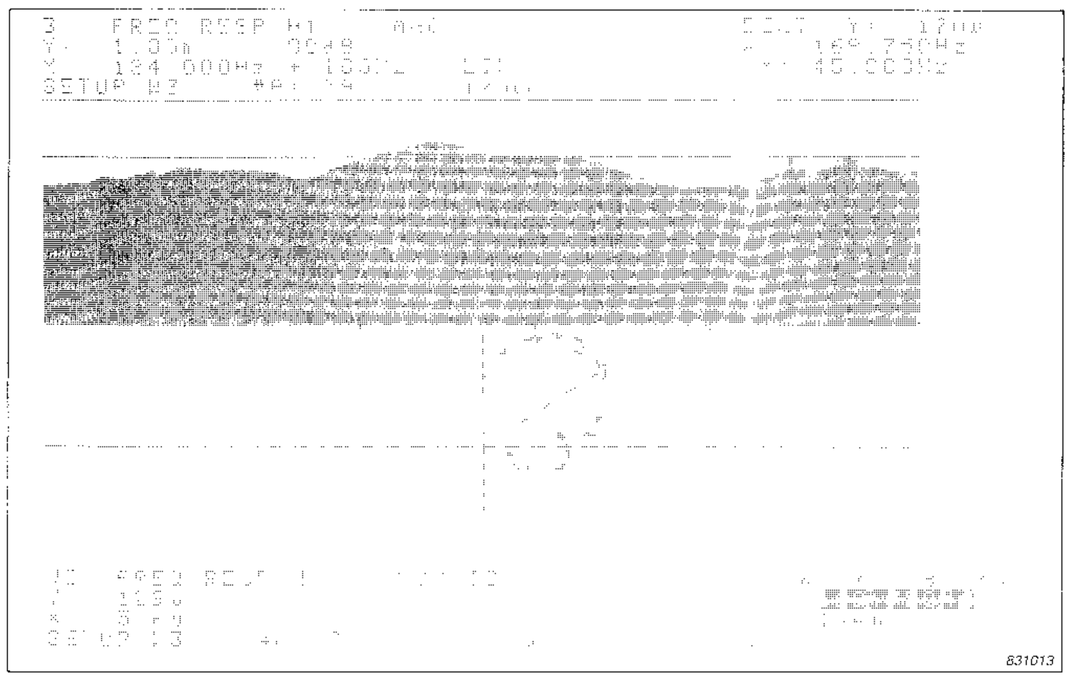

Fig. 13. Zoomed point mobility M_{AA}. Magnitude and Nyquist plot on a linear frequency scale from 124 Hz to 224 Hz

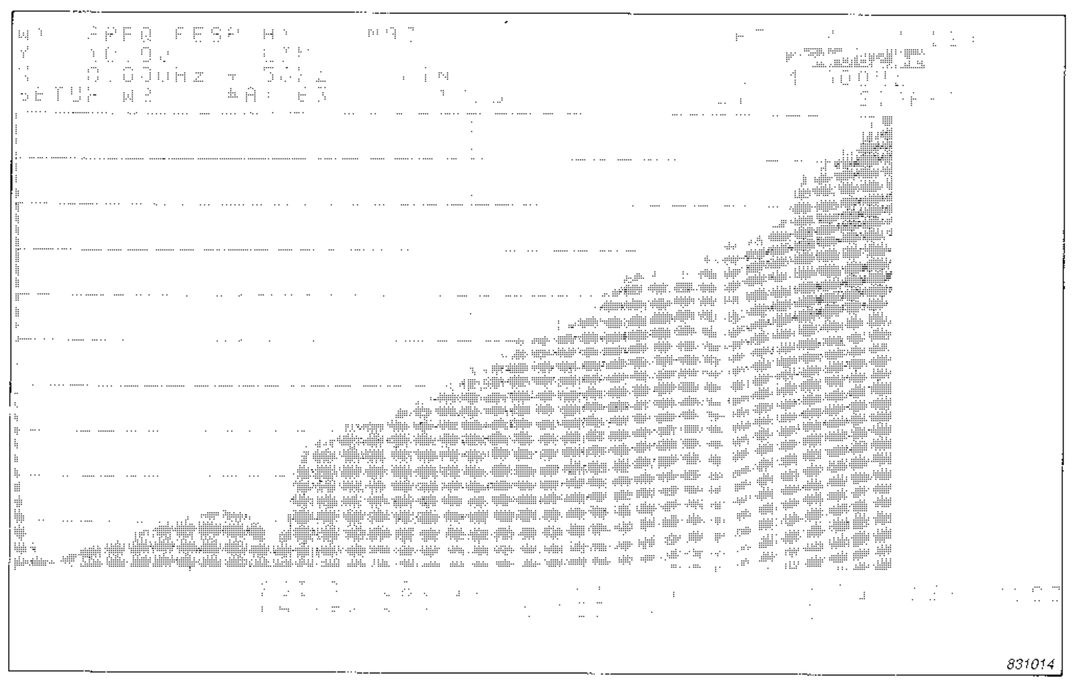

Fig. 14. Magnitude of point mobility M_{AA} on a linear / linear frequency scale over the frequency range 0 Hz to 50 Hz

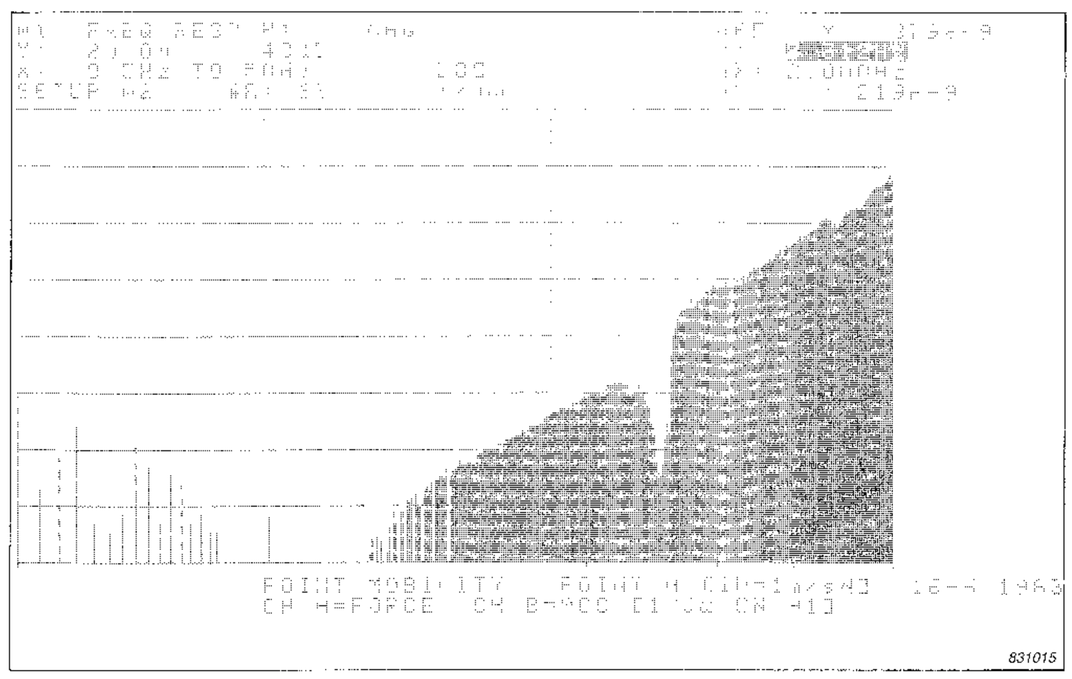

Fig. 15. Magnitude of point mobility M_{AA} on a log. / log. frequency scale from 0,5 Hz to 50 Hz

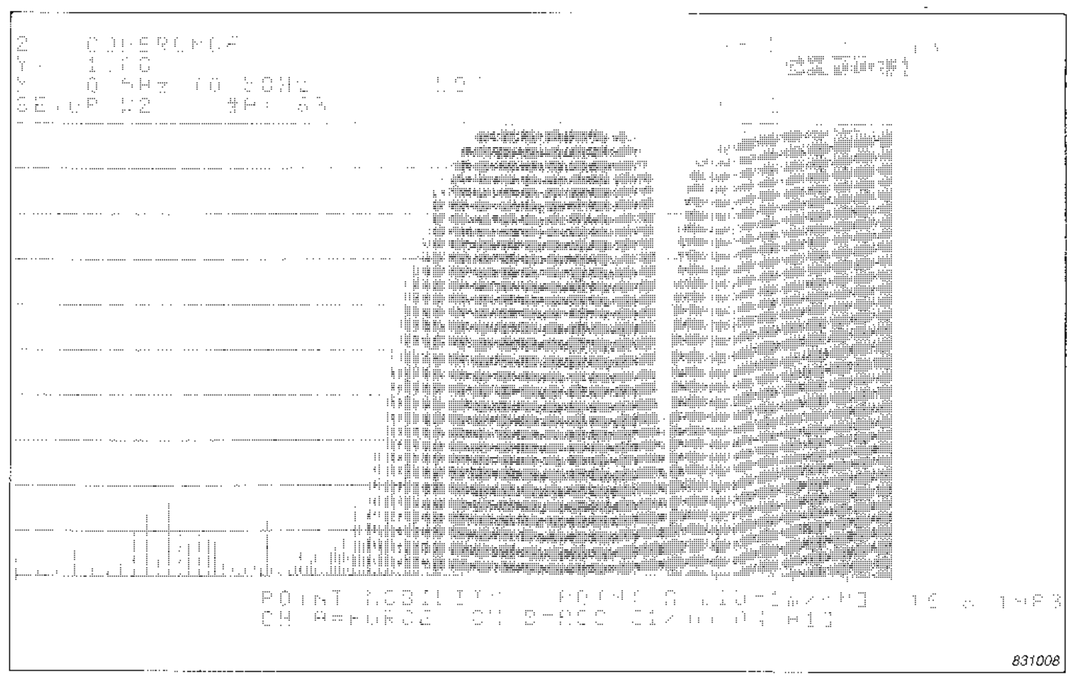

Fig. 16. Coherence of point mobility M_{AA} on a log. / log. frequency scale from 0,5 Hz to 50 Hz

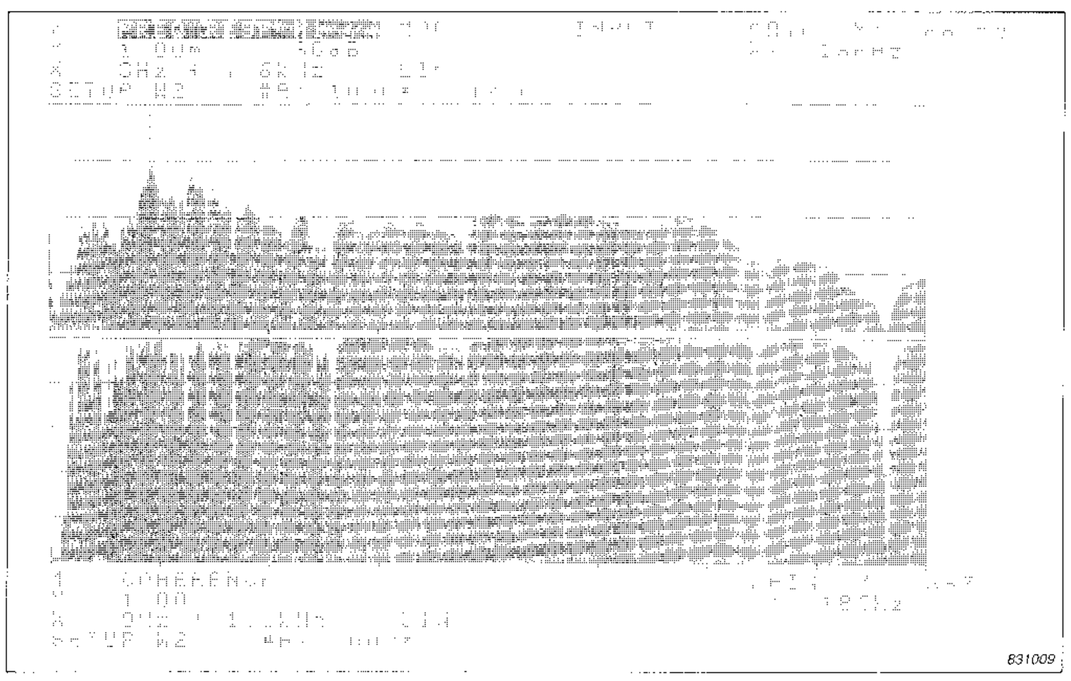

Fig. 17. Magnitude and coherence of transfer mobility M_{AB} on a linear frequency scale from 0 Hz to 1,6 kHz

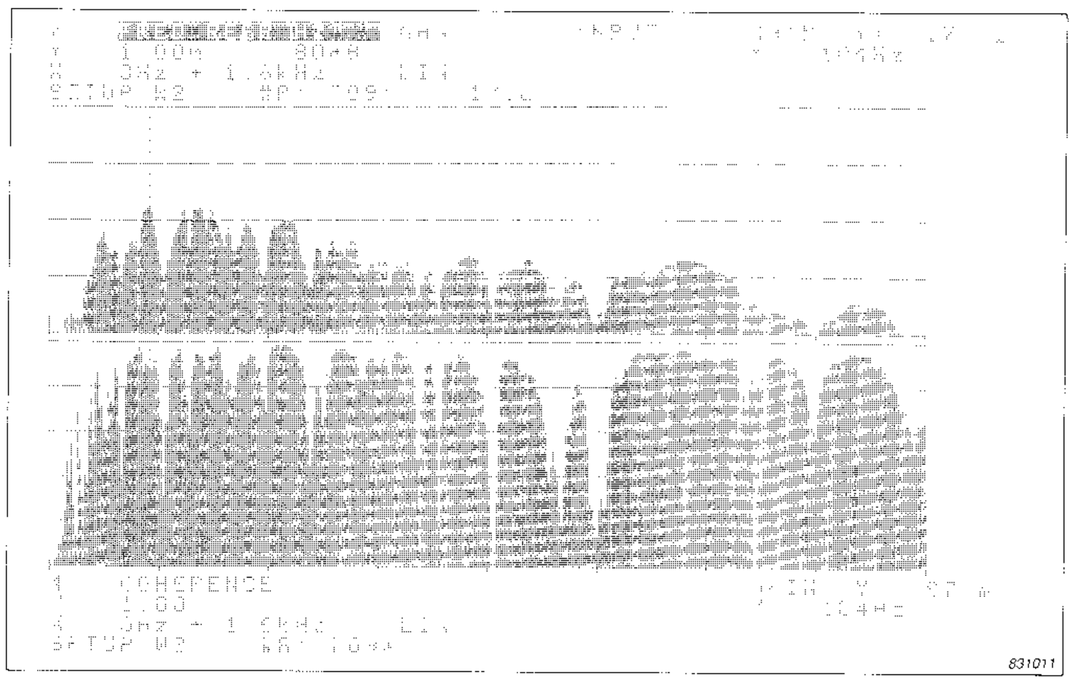

Fig. 18. Magnitude and coherence of transfer mobility M_{AC} on a linear frequency scale from 0 Hz to 1,6 kHz

system will have the same frequency response functions in both directions [9].

Measurements on workshop floor

Two parallel lines of measurement points were marked out on the floor in a direction which crossed the battens at right angles. Along one line were the points labelled 1, 2, 3 & 4 and along the other points labelled A, B & C. The interval between the measurement points was 1 m. Points 1 and C were closest to the centre of the floor and points 4 & A closest to the outer wall. Fig.4 shows the relative positions of the measurement points.

At measurement points 1, 2, 3, 4 & A, the point mobilities were measured and are denoted by M_{11}, M_{22}, M_{33}, M_{44}, M_{AA}. The transfer mobilities were measured firstly with the exciting force applied at point 1 and the velocity measured at points 2, 3 & 4, and secondly with the exciting force applied at point A and the velocity measured at points B and C. These transfer mobilities are denoted by M_{12}, M_{13}, M_{14}, M_{AB}, M_{AC}.

Coherence between the excitation and response signals was measured in all tests. Below 5 Hz the value of the coherence was low which means there is a lower statistical accuracy at these frequencies for a given number of averages.

Measurement results

Some of the measurement results are shown in Figs. 5 to 18. The point mobility at point A, M_{AA}, from 0 Hz to 400 Hz on a linear scale and 4 Hz to 400 Hz on a logarithmic scale are shown in Figs. 5 & 6. These figures also show the phase and the measurement set-up of the analyser respectively. The magnitude of the impulse response is shown in full-size format in Fig. 7. From the decay rate of this curve an estimate for the loss factor of the floor was obtained (see later section).

The most important resonances of the floor were seen to occur at frequencies below 400 Hz so most of the subsequent measurements were made at frequencies below this value. The point mobility at point A, M_{AA}, over the frequency range 80 Hz to 280 Hz and the corresponding coherence and phase are shown in Figs. 8, 9 & 10. The coherence is very close to unity over most of the frequency range, which indicates that practically all the response signal is due to the excitation signal and that there is a linear relation between the excitation and the response. The main resonances at point A are seen to be at 171 Hz and 246 Hz. The resonances at some of the other measuring points are given in Table 1.

Nyquist plot

A plot of the imaginary versus the real part of a function (either a time or a frequency function) is called a Nyquist plot. On such a plot resonances occur as nearly circular arcs. Fig. 11 shows the Nyquist plot for point A over the frequency range 160 Hz to 255 Hz. The "pig's tail" form of the Nyquist plot indicates the presence of coupled resonances.

	Point A				Point 3		Point 4				
Range Hz	**0–400**		**80–280**		**48–448**		**48–448**			**96–196**	
Resonance Hz	170	245,5	171	246,25	179	196	112	185,5	277	112	185,5
3 dB bandwidth	0,05	0,04	0,04	0,04	0,06	0,06	0,08	0,04	0,05	0,08	0,04
$\frac{d\phi}{df}$	0,10	0,05	0,06	0,06	0,08	0,08	0,10	0,05	0,06	0,09	0,04
Decay rate of mag. imp. res.	0,06		0,05		—		0,08			0,06	

Table 1. Loss factor for a wooden floor estimated in various frequency bands by different methods at three measurement points

Magnitude of impulse response

Fig. 7 shows the magnitude of the impulse response at point A from 0 Hz to 400 Hz. Let the real valued impulse response function be denoted by h(t). By employing the Hilbert transform denoted by $\mathscr{H}$ the corresponding analytic signal is given by:

$$z(t) = h(t) + i\,\mathscr{H}[h(t)]$$
$$= h(t) + i\tilde{h}(t)$$

The magnitude or envelope of the impulse response is then given by:

$$|z(t)| = \sqrt{h^2(t) + \tilde{h}^2(t)}$$

which in the domain of Time Delay Spectrometry (TDS) is called the Energy Time Curve (ETC).

Zoomed measurements

The zoom facility can be used to obtain better frequency resolution and hence a more correct measure of resonance frequency and the peak levels at resonance. The parameters for the resonance at 170 Hz at point A, for example, is better estimated from Fig. 12 than from Fig. 9. Figs. 12 & 13 show the results of zooming on the point mobility at point A, the corresponding measurement set-up and the Nyquist plot in the range 124 Hz to 224 Hz respectively.

Compliance and stiffness of the floor

Fig. 14 shows the point mobility from 0 Hz to 50 Hz on a linear / linear scale. The usefulness of the special Δx and Δy cursors on the analyser can be seen in the following simple calculation. Mobility M is related to compliance C by $M = 2\pi f C$. Therefore:

$$dM / df = 2\pi C = \Delta y / \Delta x$$

The values of $\Delta x = 4$ Hz and $\Delta y = 615 \times 10^{-9}$ are read from the top right hand corner of Fig. 14. Therefore the compliance C in the frequency range of 20 Hz to 30 Hz is $0{,}25 \times 10^{-7}$ m / N and its reciprocal i.e. the stiffness K, is $0{,}41 \times 10^{8}$ N / m.

The same data are shown on a log / log scale in Fig. 15. Here the value of the compliance C in the frequency range 8,3 Hz to 10,3 Hz is $1{,}1 \times 10^{-7}$ m / N and the stiffness K is $9{,}1 \times 10^{6}$ N / m. Fig. 16 shows a pronounced drop in coherence for this measurement at about 15 Hz which is due to the antiresonance clearly shown in the point mobility.

Transfer mobility

The transfer mobilities M_{AB} and M_{AC} and their coherences over the frequency range 0 Hz to 1,6 kHz are shown in Figs. 17 & 18. The transfer mobilities are seen to be more "ragged" in appearance and their coherences less than that of the point mobility measurements, due to a poorer signal to noise ratio at the anti-resonances. As one might expect the coherence decreases as the distance between the force transducer and the accelerometer increases.

Methods of calculating loss factor

From the mobility diagrams displayed by the Dual Channel Analyzer, the average loss factor η was estimated in various frequency bands by three different methods and the results summarised in Table 1:

1. The half power bandwidth, "3 dB points".
2. Rate of change of phase with frequency at resonance.
3. Decay rate of the magnitude of the impulse response.

Half power bandwidth, "3 dB points"

The loss factor of a particular resonance can be calculated from the bandwidth of the resonance peak in the magnitude of the mobility. If the damping is relatively small, the loss factor is given by:

$$\eta = 1 / Q = \Delta f / f_n$$

where Q is the quality factor of the resonance, Δf is the width of the resonance in Hz at points 3 dB lower than the resonance peak and f_n is the resonance frequency. The width can be found from the magnitude diagrams using the reference cursor. From Fig. 9, for the resonance at 171 Hz at point A, $\Delta f = \Delta x = 7{,}25$ Hz which gives $\eta = 0{,}04$.

Rate of change of phase with frequency

The loss factor η is related to the rate of change of phase with frequency $d\varphi / df$ by:

$$\eta = 360 / (\pi f_n |d\varphi / df|)$$

where f_n is the resonance frequency. $d\varphi / df$ can be estimated from the phase diagrams using the reference cursor and read-out of Δx and Δy. For the resonance at 171,25 Hz at point A, for example, it is seen from Fig.10 that $\Delta y = -5{,}6°$ for $\Delta x = 0{,}5$ Hz which means that:

$$|d\varphi / df| = |\Delta y / \Delta x| = 11{,}2$$

Hence $\eta = 0{,}06$. The higher value of η obtained with this method probably arises from an underestimation of the phase gradient caused by calculating this quantity over too wide a frequency band.

Decay rate of the magnitude of the impulse response

Probably the most usual method of determining loss factors of floors and partitions is that which corresponds to the measurement of the reverberation time in air. A shaker is used to excite the floor using octave or third-octave band filtered noise. When the vibration in the floor has attained a steady state, the signal to the shaker is abruptly stopped and the decay of vibration level is recorded using an accelerometer, an amplifier and a level recorder. From the decay curve the average reverberation time T of the floor at the frequency of excitation can be measured and hence the loss factor η can be obtained from the relationship:

$$\eta = 2{,}2 / fT$$

where f is the centre frequency of the noise band. A disadvantage of this method is that the decaying signal is rapidly lost in the background vibration level. A two channel analyser may often overcome this disavdvantage by calculating the impulse response of the floor from the steady state response. An average loss factor can be estimated from the decay rate D of the impulse response by:

$$\eta = D / (8{,}7 \pi f)$$

where f is the geometrical mean value of the frequency range. For a single resonance or for a high modal density (i.e. many resonances in the band of interest) the decays obtained are fairly regular and the determination of the decay rate is unambiguous. For low modal density and decoupled modes, however, the decay may appear curved or almost erratic which makes the determination of a unique η for the selected frequency range very difficult. In such a situation one should rather calculate the decay rate and from this η for a particular resonance using editing in the frequency domain. This is a standard post-processing technique in the Dual Channel Analyzer.

Conclusion

In this application demonstration, a Dual Channel Analyzer was used to gather and store on a Digital Cassette Recorder Type 7400 large amounts of mobility data *in situ* in a relatively short time. All the subsequent processing was performed back in the office by reintroducing data from the cassette recorder into the analyser.

References

1. F.J.Fahy & M.E.Westcott, "Measurement of floor mobility", J. Sound & Vib., 1978, 57(1), pp. 101-129.
2. M.White & K. Liasjø, "Measurement of mobility and damping of floors", J. Sound & Vib., 1982, 81(4), pp. 535-547).
3. ANSI S 2.31–1979. Mechanical mobility. Part I: Basic definitions and transducers.
4. ANSI S 2.32–1982. Mechanical mobility. Part II: Single-point translational excitation.
5. ANSI S 2.33–198X (in preparation). Part III: Rotational excitation at a single point.
6. ANSI S 2.34–198X (in preparation). Part IV: Steady state excitation.
7. ANSI S 2.35–198X (in preparation). Part V: Impact excitation.
8. "Vibration control (II)", R. G. White, Noise and vibration, ed. R. G. White & J. G. Walker, pp. 687-688, pub. Ellis-Horwood 1982
9. A. Granhäll, "Mech. imp. & vib. meas.: the influence of non-linearities", Dept. of Building Acoustics, Chalmers University, Göteborg, Sweden, 1981, p.9
10. B.Petersson & J.Plunt, "Structure-borne sound transmission from machinery to foundations", Dept. of Building Acoustics, Report 80-19, Chalmers University, Göteborg, Sweden.
11. "Effect of non-linearity on transfer function", N. Okubo, Sound & Vib., Nov. 1982, pp. 34 - 37

Bruel & Kjaer Instruments, Inc.

185 Forest Street, Marlborough, Massachusetts 01752 · (617) 481-7000 · TWX: 710-347-1187

World Headquarters: Nærum, Denmark. Sales and service in principal US cities and 55 countries around the world

Printed in Denmark by Nærum Offset